Civil and Environmental Engineering
Vol. 21, Issue 2, 1259-1273, DOI: 10.2478/cee-2025-0093

RESERVOIR CAPACITY ANALYSIS FOR FLOOD MITIGATION IN THE UPPER KURANJI WATERSHED

Nofra MASDAF[1,*], Bambang ISTIJONO[1], Revalin HERDIANTO[1,3]

[1] Department of Civil Engineering, Andalas University, Indonesia.
[3] Department of Civil Engineering, Andalas University and Politeknik Negeri Padang, Indonesia.
[*]corresponding author: nofra.m.71@gmail.com

Abstract

The objective of this study is to assess the hydrological behavior of the upper Kuranji River watershed to inform reservoir capacity planning for effective flood mitigation. Four probability distributions, Normal, Log-Normal, Gumbel, and Log Pearson Type III, were used to assess maximum daily rainfall data from 2002 to 2022 at the Gunung Nago and Batu Busuk stations. The results were confirmed using the Chi-Square and Kolmogorov-Smirnov tests. Flood discharge was estimated using the Nakayasu SUH and Rational Method. The most appropriate techniques were determined to be the Gumbel and Log Pearson Type III methods, which had a peak design discharge of 1,178.67 m³/s over a 100-year return period. The nine reservoirs studied have a total storage capacity of 24,258 m³, with Siratal Mustakim 2 being the largest. According to simulation results, the 2-year return term had the greatest reservoir filling time (39.31 seconds), whilst the 100-year return period had the shortest filling time (20.58 seconds). The novelty lies in combining empirical hydrological methods, statistical rainfall modeling, and theodolite-based field surveys to estimate reservoir volume for flood mitigation in complex tropical catchments. This approach offers a more accurate and practical framework for flood control planning in tropical urban watersheds with complex terrain and rapid land-use change.

Keywords:

Reservoir;
Rainfall;
Probability Distribution;
Nakayasu SUH;
Flood.

1 Introduction

Urban catchment areas such as the Kuranji River in Padang City, West Sumatra, Indonesia, continue to experience land use changes. Before the 1980s, the upstream catchment area was largely dominated by natural forests, with a small percentage consisting of agricultural land and residential areas. Since then, land use has shifted to being dominated by agriculture and infrastructure development. More rapid changes occurred following the earthquakes and tsunamis that struck Sumatra in 2004, 2007, and 2009, which posed threats to public safety. Due to its elevated location and distance from the coastline, the upstream area of the Kuranji River catchment in the eastern part is considered one of the relatively safe zones in Padang City.

Nevertheless, the Kuranji River catchment remains vulnerable to natural hazards. The combination of intense rainfall events and steep terrain in the upper watershed creates conditions conducive to flooding and landslides. Since 2012, the area has experienced two catastrophic flash flood events and multiple landslides, resulting in both human casualties and property damage. These incidents have led to the hypothesis that land use changes may be a contributing factor to such events.

Various efforts have been made to understand the conditions of the catchment area as a basis for water resource control and protection. Given that the Kuranji River is one of the main water supply sources for Padang City, the sustainability and quality of the water supply are of great importance. Preliminary studies on the main River have shown a significant increase in runoff from 2000 to 2018. Considering that the upstream area of the river is home to Andalas University and Politeknik Negeri Padang, where approximately 50,000 people reside daily, the Padang City Government has needed to ensure an adequate water supply for the community. Since 2010, several reservoirs have been constructed in the upstream area, particularly within the campus zones. Theoretically, a reservoir is a basin-shaped structure that functions to store rainwater or surface water, and it is generally used for irrigation, clean water supply, recreation, and flood control [1-5]. Reservoirs serve multiple functions beyond hydrological control, including supporting agricultural production, energy generation, domestic needs, and even social activities, making them a crucial infrastructure in both rural and urban contexts [6]. In regions prone to drought, reservoirs help regulate water flow, reduce the risk of flooding, and increase water availability. This study primarily concentrates on the application of reservoirs for flood mitigation in the upper region of the Kuranji River watershed. Additionally, these reservoirs contribute to the sustainable management of water resources. The geographical layout of the Kuranji watershed is illustrated in Fig. 1, which shows the main river channel, sub-watersheds, topographical features, and the locations of key infrastructures, including reservoirs, university campuses, and residential areas, in the upstream region.

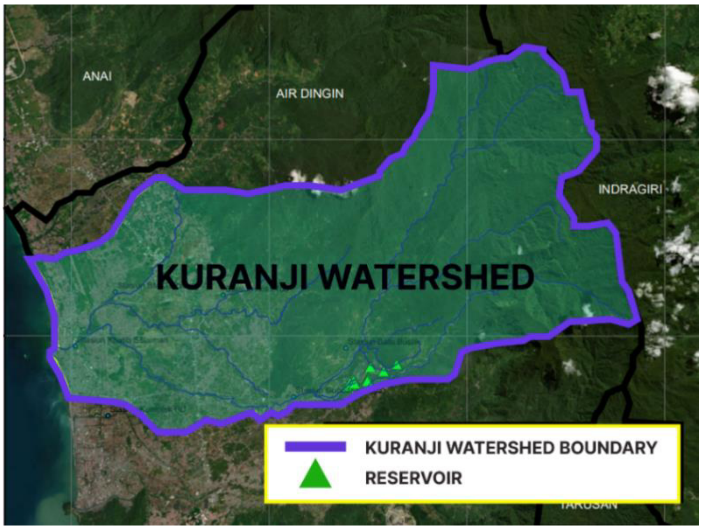

Fig. 1: Map of Kuranji Watershed.

In the upper Kuranji river watershed, nine reservoirs serve as important components of Padang City's water resources infrastructure. The locations of these reservoirs are shown in Fig. 2, which maps the distribution of all nine reservoirs within the upper Kuranji watershed. The figure highlights their proximity to residential zones, campus areas, and main river branches, emphasizing their role in flood mitigation and water supply. Their strategic placement and diverse functions make them essential to the livelihoods of local communities. West Sumatra Province is characterized by relatively high rainfall, mountainous topography, and, in some areas, regional geological features such as fault zones. For instance, the Kuranji river catchment receives between 2,000 and 3,000 mm of rain annually. These conditions affect the geohydrological dynamics of rivers in the province, which are highly susceptible to water-related damage. Rivers under such natural conditions are vulnerable to natural disasters, including riverbank landslides, flash floods, and widespread flooding that threaten the lives of people living along the riverbanks.

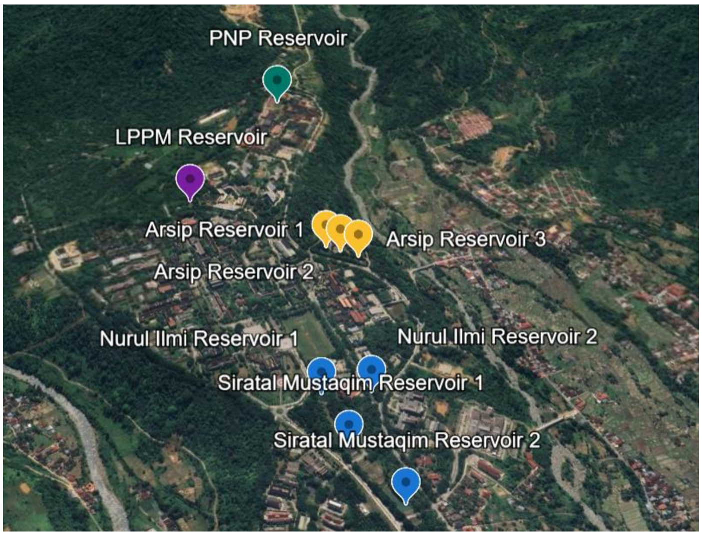

Fig. 2: Reservoirs Location Map. Source: Google Earth. (2025). Reservoirs Location Map. Retrieved June 01, 2025, from https://earth.google.com/earth/d/1eNqUQv-adpTYcT06ijcwkkhKB4RAJGjq

Stretching roughly 35 km from the mountain peaks (1,600 meters above sea level) in the east to the Indian Ocean in the west, the Kuranji River watershed occupies an area of 210 km². The watershed's upstream region includes residential neighborhoods, campus zones, agricultural land, natural rainforest, and nine strategically positioned reservoirs that have been constructed since 2010 and significantly lower the risk of flooding. Because of the high terrain and significant changes in land use, hydrological analysis requires a more creative methodology [7].

In order to assist empirically-based flood management planning, this study combines field data gathered with a theodolite with hydrological modeling and statistical rainfall analysis with the Nakayasu SUH method. The initial dataset consists of maximum daily rainfall records from the Gunung Nago and Batu Busuk stations for the period 2002–2022. From this data, the average annual daily rainfall was calculated. Four probability distributions were employed to calculate rainfall probabilities (in millimeters) for different return periods: The Chi-Square [8] and Kolmogorov-Smirnov [9] tests were used to validate the Normal, Log-Normal, Gumbel, and Log Pearson Type III tests [10-13]. To find the best approach for calculating design flood discharge and peak runoff in the research area, stream discharge was computed using the Nakayasu SUH and the Rational Method.

Reservoirs play a crucial role in flood mitigation in areas with high rainfall and rapid land-use changes. Previous studies have addressed flood operation optimization for complex systems using advanced modeling approaches. In [14], a dual-objective optimization approach was proposed for a five-reservoir system to develop optimal flood control operation rules in the Chaobai River Basin. Nevertheless, the model depends heavily on simulation-optimization cycles and detailed flood operation policies. To address challenges in less complex but highly variable tropical environments, this study applies an empirical-based approach combining hydrologic probability analysis and field-based topographic measurements. This method is specifically tailored for flood control planning in the Upper Kuranji watershed.

2 Research Methods

This section outlines the methodological steps and strategies employed in the study to assess reservoir capacity in the Upper Kuranji River watershed. The approach integrates topographic measurements for reservoir volume estimation, rainfall frequency analysis, probability distribution testing, and flood discharge calculation. Each method is designed to ensure accuracy and relevance in planning flood control infrastructure. The methodology is structured in four main stages as described below.

2.1 Reservoir Capacity

The first stage involves determining the storage volume of the reservoirs using field-based measurements and spatial analysis. Direct measurements were carried out using a theodolite, as the depth of the reservoirs being assessed could still be accurately measured with this instrument, unlike several similar studies that used bathymetric surveys to determine reservoir depth. The data obtained were then processed using the contour method to calculate the reservoir storage volume, a widely applied technique in hydrological and topographical analyses for estimating the volume between successive elevation contours [15].The volume calculation using the contour method can be performed using the following formula:

$$\boldsymbol{V} = \Delta\boldsymbol{H}\,(\boldsymbol{n}-\boldsymbol{1})\frac{\sum_{i=1}^{n}\boldsymbol{Li}}{\boldsymbol{n}} \tag{1}$$

where:

- $\boldsymbol{V}$ - peak discharge [m^3/s],
- $\Delta\boldsymbol{H}$ - contour interval [m],
- n - number of contour lines,
- $\boldsymbol{Li}$ - inundation area at the i-th contour line [m^2].

2.2 Analysis of Rainfall Data

To complement the volume estimation, rainfall data analysis is conducted to evaluate the likelihood of extreme precipitation events [16]. This step is essential in understanding the hydrological inputs affecting reservoir inflow. Rainfall frequency analysis was conducted to determine the probability of extreme rainfall events that could potentially lead to flooding [15-18]. This step is crucial in planning flood control infrastructure, such as reservoirs, as it enables the prediction of rainfall for various return periods. In this study, maximum daily rainfall data served as the basis for the calculations. Four probability distribution techniques are then used to examine the data. The best-fitting distribution was selected using the goodness-of-fit tests.

2.2.1 Normal Distribution Method

Rainfall data that exhibit a symmetrical distribution around the mean are commonly modeled using the normal distribution, one of the most widely applied continuous probability distributions in hydrological research [19-21]. The normal distribution, also referred to as the Gaussian distribution or bell curve, serves as a valuable approximation for numerous natural phenomena that display random variation around a central tendency. Temperature, relative humidity, and wind speed are just a few of the hydrological variables that have a normal distribution [22]. The equation is used to determine the normal distribution approach:

$$F(x) = \frac{1}{\sqrt{2\pi\sigma^2}}\int_{-\infty}^{x} e^{-(t-\mu)^2/(2\sigma^2)}dt \tag{2}$$

$$\mu = \bar{x} \tag{3}$$

$$\sigma = S_x \tag{4}$$

where:

$F(x)$ - cumulative distribution function (CDF) of the rainfall variable at value x,
μ - average of the rainfall information,
σ - rainfall data standard deviation,
t - dummy variable for integration,
π - Pi constant [$\approx 3,1416$],
e - natural exponential constant [$\approx 2,71828$].

2.2.2 Log Normal Distribution Method

When rainfall data exhibit uneven distribution, characterized by predominantly modest to moderate values with occasional sporadic heavy rainfall events significantly exceeding typical amounts, the two-parameter log-normal distribution is often utilized due to its proven ability to model positively skewed hydrological data [19-20],making it a suitable choice for representing such variability in rainfall patterns.. This continuous probability distribution effectively models random variables that become normally distributed upon applying a logarithmic transformation [22]. The equation is used to calculate the log-normal distribution approach:

$$F(x) = \int_{0}^{x} \frac{1}{t\sigma_y\sqrt{2\pi}} e^{-(ln(t)-\mu_y)^2/(2\sigma_y^2)}dt \tag{5}$$

$$\mu_y = \bar{y} \tag{6}$$

$$\sigma_y = S_y \tag{7}$$

where:

μ_y - mean of the logarithmically transformed rainfall data [i.e., y = ln(x)],
σ_y - standard deviation of the logarithmically transformed rainfall data,
$\ln(t)$ - natural logarithm of t.

2.2.3 Gumbel Method

The Gumbel distribution was selected in this study due to its recognized effectiveness in modeling annual maximum rainfall and extreme hydrological events [19-25]. Its statistical performance, indicated by a low Chi-Square value and acceptable deviation in the Kolmogorov–Smirnov test, further supports its suitability for estimating design rainfall, especially in flood-prone and topographically complex areas such as the Upper Kuranji Watershed. Planning for flood control commonly involves the analysis of extreme events, including annual maximum rainfall, using the Gumbel method due to its ability to characterize tail behavior in hydrological extremes. The kind of extreme value distribution is the Gumbel distribution, which was developed by Gumbel. This type of distribution is typically applied in the analysis of variables like watershed discharge, as well as the maximum 24-hour rainfall recorded on a monthly or annual basis [22]. The Gumbel method is calculated using the equation:

$$F(x) = e^{\pm e^{\frac{\pm(x-\beta)}{\alpha}}} \tag{8}$$

$$yi = -ln\left(ln\left(\frac{1+N}{i}\right)\right) \tag{9}$$

$$\alpha = \frac{S_x}{\sigma_y} \tag{10}$$

where:

β - location parameter, typically estimated from the mean of the data,
α - scale parameter, representing the spread of the data,

S_x - rainfall data standard deviation,
σ_y - Gumbel distribution's standard deviation,
y_i - reduced variate at the i-th rank,
i - data rank, arranged from top to lowest,
N - total amount of data points observed,
ln - natural logarithm.

2.2.4 Log Pearson Type III Method

The Log Pearson Type III distribution was also used because it is well-suited for modeling skewed rainfall data. This method showed strong statistical conformity in both Chi-Square and Kolmogorov–Smirnov tests, and it produced the highest rainfall estimates across all return periods, making it appropriate for conservative flood control planning. This technique is widely used in hydrological research because it can handle severe rainfall data, which often has a skewed distribution with many low values and a few exceptionally high ones [22]. This equation is employed to perform calculations using the Log Pearson Type III method

$$F(x) = \frac{1}{\beta^{\alpha}\Gamma(\alpha)}\int_{e^{x_0}}^{x}\frac{(ln(t)-x_0)^{\alpha-1}e^{-(1n(t)-x_0)/\beta}}{t}dt \quad (11)$$

$$F(y) = \frac{1}{\Gamma(\alpha)}\int_{0}^{y}u^{\alpha-1}e^{-u}du \quad (12)$$

$$\alpha = \frac{4}{C_s^2(z)} \quad (13)$$

$$\beta = \frac{C_s(z)S_z}{2} \quad (14)$$

$$x_0 = \bar{z} - \frac{2S_z}{C_s(z)} \quad (15)$$

where:
t - integration variable of the rainfall value in the logarithmic domain,
ln(t) - natural logarithm of the rainfall value,
$\Gamma(\alpha)$ - gamma function of the shape parameter α,
α - shape parameter, dependent on the skewness coefficient,
β - scale parameter, determined by the standard deviation and skewness,
x_0 - location parameter, calculated from the mean of the log-transformed data,
$C_s(z)$ - skewness coefficient of the logarithmic rainfall data,
S_z - standard deviation of the logarithmic rainfall data,
$\bar{z}$ - mean of the logarithmic rainfall data,
$F(y)$ - general integral form of the Pearson Type III distribution,
u - dummy variable for gamma integration.

2.3 Probability Distribution Testing

Following rainfall frequency analysis, probability distribution testing is conducted to determine the statistical distribution that best represents the observed data. This step is essential to ensure the accuracy and reliability of rainfall estimates used in subsequent hydrological modeling processes. The result from the greatest discrepancy between the observed and theoretical cumulative density function is obtained using the Kolmogorov-Smirnov method. However, Chi-Square accounts for the discrepancy between observed and expected frequencies [22], [26]. Probability distribution tests are essential in rainfall frequency analysis to identify the distribution that best represents annual maximum rainfall patterns. This ensures accurate estimation of design rainfall for specific return periods. Annual maximum rainfall data undergo frequency analysis and are compared against various distribution models, with the best fit selected based on the lowest statistical error. Subsequently, these results inform the calculation of discharge entering the reservoirs.

2.4 Design flood discharge

Based on the selected rainfall distribution, the design flood discharge is calculated by correlating rainfall intensity with potential flood volumes to assess reservoir capacity for effective flood mitigation. Following rainfall frequency analysis and probability distribution testing, the next step is to determine the design discharge using the Rational method and the Nakayasu Synthetic Unit Hydrograph (SUH). Although each method has different assumptions and calculation techniques, both are essential for providing a comprehensive understanding of potential water flow in the upper Kuranji River watershed. The upstream region of the Kuranji River watershed's land use patterns and soil types are taken into account when adjusting the runoff coefficients used in the Rational Method and the Nakayasu SUH to calculate discharge [27,28]. These coefficients indicate the fraction of rainfall that transforms into surface runoff and play a crucial role in ensuring the accuracy of peak discharge estimations. The runoff coefficient values presented in Table 1 were selected based on observed land cover types and soil conditions in the Upper Kuranji Watershed [17]. For paved residential areas, a runoff coefficient of 0.70 was used, reflecting observed land cover and soil type.

Table 1: Runoff Coefficients (C). Source: [17]

Land Cover	C	Land Cover	C
Business		**Lawns, Sandy Soil**	
Downtown	0.70 – 0.95	Flat, 2 %	0.05 – 0.10
Neighborhood	0.50 – 0.70	Average, 2% - 7 %	0.10 – 0.15
Residential		Steep, > 7%	0.15 – 0.20
Single-family	0.30 – 0.50	**Lawns, heavy soil**	
Multiunits, detached	0.40 – 0.60	Flat, 2 %	0.17 – 0.17
Multiunits, attached	0.60 – 0.75	Average, 2% - 7 %	0.18 – 0.22
Residential (suburban)	0.25 – 0.40	Steep, > 7%	0.25 – 0.35
Industrial		**Agricultural area**	
Light	0.50 – 0.80	Open land	
Heavy	0.60 – 0.90	Flat	0.30 – 0.60
Parks, cemeteries	0.10 – 0.25	Rough	0.20 – 0.50
Playgorund	0.30 – 0.35	**Cultivated area**	
Railroad yard	0.20 – 0.35	Heavy soil, no vegetation	0.30 – 0.60
Unimproved	0.10 – 0.30	Heavy soil, vegetation	0.20 – 0.50
Pavements		Sandy soil, no vegetation	0.20 – 0.25
Asphalt	0.70 – 0.85	Sandy soil, vegetation	0.10 – 0.25
Concrete	0.70 – 0.95	**Meadow**	
Stone/Brick	0.70 – 0.85	Heavy Soil	0.15 – 0.45
Pedestrian	0.75 – 0.85	Sandy Soil	0.05 – 0.25
Roofs	0.75 – 0.95	Forest, Vegetation	0.05 – 0.25
		Bare land	
		Flat, impervious	0.70 – 0.90
		Rough	0.50 – 0.70

2.4.1 Rational Method

In flood control planning, one of the methods used to calculate runoff discharge is the Rational Method. This method is particularly useful for estimating peak discharge in watersheds that have sufficient rainfall data, specifically data that is recorded continuously and is representative over a certain period (at least 10 years), allowing it to reflect the rainfall pattern occurring in the region. The runoff discharge is calculated by using the equation of the rational method [26-32]. Peak discharge is calculated using the following formula:

$$Qp = 0{,}278\,.C.I.A \tag{16}$$

where:

$\boldsymbol{Qp}$ - maximum flood flow rate [m^3/s],
$\boldsymbol{C}$ - coefficient,
$\boldsymbol{I}$ - intensity of the rainfall during the focus period [mm/h],
$\boldsymbol{A}$ - area of the watershed [hectares].

In addition to the Rational Method, another hydrological modeling approach, the Nakayasu SUH employed to cross-validate the discharge estimates and provide a more robust analysis.

2.4.2 Nakayasu SUH

As an alternative method for estimating peak discharge, the Nakayasu SUH [33,34] approach is employed to calculate peak flow through an empirical framework. This method is particularly effective in characterizing the hydrological response of a watershed to extreme rainfall events by utilizing a unit hydrograph that reflects the specific physical and hydrological characteristics of the region. One of the well-known empirical formulas for calculating peak runoff rates is provided by the Nakayasu SUH approach. Typical hydrographs for a certain watershed are called unit hydrographs [35,36]. Peak discharge is determined using the formula below:

$$Qp = \frac{C\ A.R_0}{3{,}6\ (0{,}3\ T_p + T_{0,3})} \tag{17}$$

where:

$\boldsymbol{R}$ - unit rainfall,
$\boldsymbol{T_p}$ - rainfall intensity during the time of concentration [mm/h],
$\boldsymbol{T_{0,3}}$ - time of discharge to drop from its maximum to 30% of its maximum.

3 Data Analysis

This section outlines the data processing and interpretation methods employed in the study. The analysis integrates rainfall data, reservoir capacities, and design flood discharge estimations using the Nakayasu SUH and Rational methods to evaluate the interaction between runoff, rainfall intensity, and storage capacity in mitigating flood risk within the study area.

3.1 Rainfall Data

The rainfall data used in this study are deemed highly relevant and representative of the hydrological conditions in the Upper Kuranji River watershed. Sourced from Gunung Nago and Batu Busuk Stations, the data show substantial year-to-year variability, with average daily rainfall ranging from 118 mm (2010) to 231.6 mm (2005). Gunung Nago Station generally recorded higher rainfall than Batu Busuk. No consistent temporal trend was observed due to significant annual fluctuations. Table 2 presents a detailed summary of the annual rainfall data.

Table 2: Rainfall Data.

No.	Year	Daily Rainfall		Average Daily Rain [mm]
		Gunung Nago Station [mm]	Batu Busuk Station [mm]	
1	2002	186.00	145.00	165.50
2	2003	186.00	155.00	170.50
3	2004	186.00	155.00	170.50
4	2005	270.20	193.00	231.60
5	2006	270.20	105.00	187.60
6	2007	98.00	175.00	136.50
7	2008	239.00	155.00	197.00
8	2009	196.00	87.00	141.50
9	2010	180.00	56.00	118.00
10	2011	170.00	115.00	142.50
11	2012	140.00	145.00	142.50
12	2013	191.00	169.00	180.00
13	2014	139.00	133.00	136.00
14	2015	231.00	191.00	211.00
15	2017	241.00	199.00	220.00
16	2018	146.00	142.00	144.00
17	2019	126.00	140.00	133.00
18	2020	231.00	202.00	216.50
19	2021	260.80	189.00	224.90
20	2022	256.00	187.00	221.50

3.2 Reservoir Storage Capacity

Based on field measurements and topographic analysis using the contour method, the storage capacity data for the nine reservoirs distributed across the study area were obtained. The calculations were performed by considering the surface area and elevation of each reservoir to determine the available water storage volume. The calculation results show that Embung Siratal Mustakim 2 has the largest capacity, which is 14,400 m³. The total capacity of all the reservoirs calculated is 24,258 m³, as presented in Table 3.

Table 3: Reservoir Storage Capacity.

No.	Reservoir Name	Storage [m^3]
1	PNP	2,418
2	LPPM	445
3	Arsip 1	1,392
4	Arsip 2	522
5	Arsip 3	1,106
6	Nurul Ilmi 1	1,141
7	Nurul Ilmi 2	1,176
8	Siratal Mustakim 1	1,653
9	Siratal Mustakim 2	14,400
	Total Storage	24,258

4 Results And Discussion

This section presents the findings of a rainfall frequency analysis carried out at two locations within the upper Kuranji River watershed: Gunung Nago Station and Batu Busuk Station. The design rainfall for various return periods was estimated using four different probability distribution methods. A goodness-of-fit test was applied to identify the most suitable distribution for the observed data. Subsequently, flood design analysis was performed based on the derived design rainfall values. The discussion concludes with an analysis of reservoir filling time based on design flood flow, which forms the basis for evaluating the effectiveness of the reservoir design in the study region.

4.1 Results of Frequency Analysis of Rainfall Data

Frequency analysis was performed on the collected rainfall data using several statistical models, including the Normal, Log-Normal, Gumbel, and Log-Pearson Type III distributions. These methods enabled the identification of rainfall probability distributions and the estimation of rainfall intensities for various return periods.

4.1.1 Normal Distribution Method

The results of the rainfall frequency analysis using the Normal Distribution method are summarized in Table 4. The calculated mean rainfall ($\bar{X}$) is 174.53 mm, with a standard deviation (S) of 36.20 mm. Rainfall estimates for various return periods were derived as follows: 204.93 mm for a 5-year return period, 220.86 mm for 10 years, 236.43 mm for 25 years, 248.73 mm for 50 years, and 258.87 mm for 100 years. These estimates were obtained by applying distinct frequency factors (Kt) associated with each respective return period.

Table 4: Normal Method Arithmetic Calculation Results.

No.	Return Period [year]	$\bar{X}$ [mm]	Kt	S [mm]	XT [mm]
1	2	174.53	0.00	36.20	174.53
2	5	174.53	0.84	36.20	204.93
3	10	174.53	1.28	36.20	220.86
4	25	174.53	1.71	36.20	236.43
5	50	174.53	2.05	36.20	248.73
6	100	174.53	2.33	36.20	258.87

Projected rainfall value increases with the length of the return period.This suggests that while extreme rainfall events are less frequent, they have a bigger effect when they do happen. Consequently, this knowledge is essential for managing and planning water resources, particularly when creating infrastructure that can withstand heavy rains.

4.1.2 Log Normal Distribution Method

Table 5 displays the findings of the rainfall frequency computation utilizing the Log-Normal Distribution approach. The log standard deviation (S Log X) is 0.09, and the log-mean rainfall value (Log $\bar{X}$) is 2.23. The rainfall depths associated with return periods of 5, 10, 25, 50, and 100 years were estimated as follows: They are 204.36 mm, 224.48 mm, 246.06 mm, 264.58 mm, and 280.87 mm in that sequence. These figures were calculated by analyzing a large number of return periods. These numbers were calculated by logarithmically converting the data and using the frequency factor (Kt) appropriate for each return period.

Table 5: Results of Arithmetic Calculation of Log Normal Method.

No.	Return Period [year]	Log $\bar{X}$ [log mm]	Kt	S Log X [log mm]	Log Xt [log mm]	XT [mm]
1	2	2.23	0.000	0.09	2.23	170.82
2	5	2.23	0.840	0.09	2.31	204.36
3	10	2.23	1.280	0.09	2.35	224.48
4	25	2.23	1.710	0.09	2.39	246.06
5	50	2.23	2.050	0.09	2.42	264.58
6	100	2.23	2.330	0.09	2.45	280.87

Extreme rainfall events are less frequent but typically have a big influence, as evidenced by the rise in rainfall values as the return period lengthens. Rainfall data, which is usually not symmetrically distributed, can be more accurately modeled by using the Log-Normal distribution. As a result, these computational findings can be used to plan drainage systems, flood prevention, and infrastructure for sustainable water resource management.

4.1.3 Gumbel Method

Table 6 presents the results of the rainfall frequency analysis conducted using the Gumbel Distribution method. The mean rainfall value ($\bar{X}$) applied in the calculations is 174.53 mm, accompanied by a standard deviation (S) of 36.20 mm. Rainfall estimates for different return periods were determined as follows: 209.52 mm for a 5-year return period, 236.13 mm for 10 years, 267.15 mm for 25 years, 294.68 mm for 50 years, and 319.43 mm for 100 years. These values were derived by utilizing the Gumbel frequency constant (Kt), which is calculated based on the standardized deviation (Sn) and the reduction variables (Yt and Yn) corresponding to each return period analyzed.

Table 6: Results of Arithmetic Calculation of Gumbel Method.

No.	Return Period	$\bar{X}$ [mm]	Yt	Yn	Sn	Kt	Sx (mm)	XT [mm]
1	2	174.53	0.3065	0.5128	1.0210	-0.2021	36.20	167.22
2	5	174.53	1.4999	0.5128	1.0210	0.9668	36.20	209.52
3	10	174.53	2.2504	0.5128	1.0210	1.7019	36.20	236.13
4	25	174.53	3.1255	0.5128	1.0210	2.5590	36.20	267.15
5	50	174..53	3.9019	0.5128	1.0210	3.3194	36.20	294.68
6	100	174.53	4.6001	0.5128	1.0210	4.0032	36.20	319.43

The Gumbel distribution is known to be effective for modeling extreme events, such as maximum rainfall. The calculation results show a trend of increasing rainfall values as the return period lengthens, reflecting a higher potential risk of flooding during low-probability rainfall events. Therefore, this information is highly useful in supporting technical decisions in the planning of dams, drainage channels, and long-term flood control systems.

4.1.4 Log Pearson Type III Method

Table 7 summarizes the results of the rainfall frequency analysis performed using the Log Pearson Type III distribution method. The logarithmic mean rainfall (Log $\bar{X}$) is 2.23, with a logarithmic standard deviation (S Log X) of 0.09. The estimated rainfall amounts for return periods of 5, 10, 25, 50, and 100 years are 189.21 mm, 221.63 mm, 277.30 mm, 331.05 mm, and 395.21 mm, respectively. These values were calculated by applying frequency factors (Kt) corresponding to each return period after logarithmic transformation of the rainfall data.

Table 7: Results of Arithmetic Calculation of Log Pearson Type III Method.

No.	Return Period [year]	Log $\bar{X}$	KT	S Log X	Log Xt	XT [mm]
1	2	2.23	0	0.09	2.23	170.82
2	5	2.23	0,48	0.09	2.28	189.21
3	10	2.23	1.22	0.09	2.35	221.63
4	25	2.23	2.27	0.09	2.44	277.30
5	50	2.23	3.10	0.09	2.52	331.05
6	100	2.23	3.93	0.09	2.60	395.21

Log Pearson Type III distribution is often used in hydrological studies because it can handle skewed or asymmetric rainfall data. The computing findings show that when the return period lengthens, rainfall levels dramatically rise. This illustrates how, despite their rarity, heavy rainstorm events with extremely high precipitation have a significant probability of happening. Thus, the use of this technique is essential for planning flood control systems, developing water infrastructure, and reducing the danger of hydrometeorological disasters.

The estimated rainfall amounts for a 25-year return period differ depending on the probability distribution method applied in the study. Using the Normal distribution, the rainfall is calculated at 236.43 mm, while the Log-Normal approach yields 246.06 mm. The highest estimate of 277.30 mm is obtained from the Log Pearson Type III method, whereas the Gumbel method produces a slightly lower value of 267.15 mm. Figure 3 depicts the relationship between rainfall intensity and return period by plotting design rainfall values for various return periods derived from four probability distribution methods: Normal, Log-Normal, Gumbel, and Log-Pearson Type III. The figure reveals that the Log-Pearson Type III method consistently yields the highest rainfall intensity estimates across all return periods, whereas the Normal distribution produces the lowest. Additionally, the divergence among the curves becomes more pronounced with increasing return periods, highlighting the significant impact that the choice of distribution has on rainfall estimation.

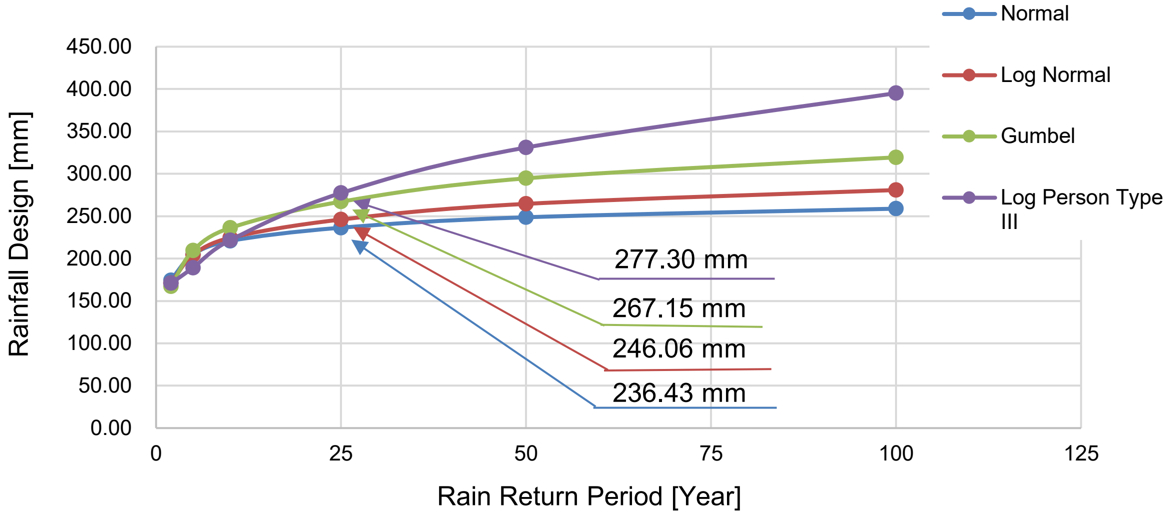

Fig. 3: The Rainfall Design and Rain Return Period Relationship Graph.

Variation in rainfall values between approaches illustrates how sensitive each method is to the properties of the data. Due to their greater sensitivity to extreme values, the Log Pearson Type III and Gumbel approaches typically yield better results. The Normal and Log-Normal approaches, on the other hand, yield more conservative outcomes. As a result, the planning goals and the allowed degree of risk should be taken into consideration while choosing the best approach. Approaches that take extreme events into account, such as Gumbel or Log Pearson Type III, are highly advised for planning vital infrastructure, like dams or major drainage systems.

4.2 Probability Distribution Testing Results

Following the rainfall frequency analysis using multiple probability distribution methods, a distribution fit test is conducted to evaluate the appropriateness of the selected models for representing historical rainfall data. This study utilizes two statistical tests the Chi-Square test and the Kolmogorov-Smirnov test to assess the goodness of fit, ensuring that the probability distributions accurately reflect the observed rainfall patterns.

4.2.1 Chi-Square Method

A probability distribution test was conducted using the Chi-Square test method to evaluate the fit between the historical rainfall data and the theoretical distribution used. According to the findings, both the Normal and Log-Normal approaches were rejected since their computed Chi-Square values of 6.50 were higher than the critical value of 5.991. Because the Gumbel and Log Pearson Type III techniques yielded a Chi-Square value of 2.00, which is below the critical value, the distributions are accepted and judged suitable for the data. Table 8 displays the complete results of the Chi-Square test.

Table 8: Chi-Square Test Results.

Methods	Normal	Log Normal	Gumbel	Log Pearson III
Calculated Chi-Square [χ^2]	6.500	6.500	2.000	2.000
Critical Chi-Square [χ^2cr]	5.991	5.991	5.991	5.991
Note	Not accepted	Not accepted	Accepted	Accepted

Test's findings demonstrate that not all probability distributions are suitable for correctly describing rainfall data. Since they can characterize the features of extreme and asymmetrically distributed data, the Gumbel and Log Pearson Type III approaches turn out to be more appropriate. Therefore, the use of these two distributions is more recommended for determining planned rainfall, especially for planning purposes that require precise estimates of high-intensity rainfall events. Validating the distribution model through statistical tests such as the Chi-Square is crucial so that technical decisions made based on data have a solid foundation and can be held accountable.

4.2.1 Kolmogorov Smirnov Method

To offer extra confirmation for choosing the best distribution, the probability distribution fit test was carried out utilizing the Kolmogorov-Smirnov test method in addition to the Chi-Square test. According to the test results, both the Normal and Log-Normal approaches are rejected since their computed statistic values, 0.466 and 0.309, respectively, are higher than the critical value of 0.29. The Gumbel approach, on the other hand, produced a calculated statistic value of 0.333, which is marginally higher than the critical value; however, given the tolerance for erroneous interpretation, this result is still deemed acceptable in this test. Table 9 displays the complete findings of the Kolmogorov-Smirnov test.

Table 9: Kolmogorov Smirnov Test Results.

Methods	Normal	Log Normal	Gumbel	Log Pearson Type III
Calculated Chi-Square [χ^2]	0.466	0.309	0.333	1.239
Critical Chi-Square [$\chi^2 cr$]	0.290	0.290	0.290	0.290
Remark	Not accepted	Not accepted	Accepted	Accepted

Use of the Kolmogorov-Smirnov test as a complement to the Chi-Square test provides a more comprehensive validation of the distribution fit. Although the statistical value of the Gumbel method slightly exceeds the critical limit, this distribution is still considered to adequately represent the data in the context of hydrological analysis, especially because the tolerance for small deviations is acceptable in engineering practice. The Gumbel and Log Pearson type III techniques remain the leading candidates for selecting planned rainfall distributions because of their exceptional performance in both statistical tests.

4.3 Flood Design

The analysis of rainfall probability distributions, supported by goodness-of-fit tests using the Chi-Square and Kolmogorov-Smirnov methods, reveals that the Gumbel and Log-Pearson Type III distributions most effectively represent the rainfall patterns in the study area. As a result, flood design calculations are based on the projected rainfall values generated from these two distributions. The Nakayasu SUH Method and the Rational Method are commonly employed approaches for estimating peak flood flows, which are essential for designing flood control infrastructure such as reservoirs.

4.3.1 Rational Method

Another technique for calculating flood design is the Rational Method, which takes into account the catchment area (A), rainfall intensity (I), runoff coefficient (C), and predicted rainfall (Xt) to compute the peak flood flow (Q). The computer findings show that as the return duration increases, so do the expected rains and the resulting flood flow. The projected flood discharge is 514.53 m^3/second for a two-year return period and 846.04 m^3/second for a one-hundred-year return period. The full outcomes of the flood design calculations utilizing the Rational Method are shown in Table 10.

Table 10: Rational Method Flood Design.

T	Xt [mm]	C	I [mm/hour]	A [km^2]	Q [m^3/s]
2	170.82	0.70	21.85	121.00	514.53
5	204.36	0.70	26.14	121.00	615.56
10	224.48	0.70	28.72	121.00	676.18
25	246.06	0.70	31.48	121.00	741.17
50	264.58	0.70	33.85	121.00	796.96
100	280.87	0.70	35.93	121.00	846.04

Increased hydrological risk that needs to be taken into account when planning water infrastructure is reflected in the rise in peak flood discharge with the lengthening return period. The Rational Method offers a straightforward yet efficient way to estimate flood discharge, especially in small to medium catchment areas and in places with little data. To build drainage channels, bridges, and flood control structures to endure long-term severe occurrences, this knowledge is essential.

4.3.2 Nakayasu SUH Method

In contrast to the rational method, flood designs were also calculated using the Nakayasu SUH technique. This method takes into account both the physical characteristics of the watershed and the runoff response to expected rainfall in order to calculate the peak flood flow. According to the analysis's findings, for every return period, the discharge values derived from the Nakayasu SUH approach are often greater than those derived from the Rational approach. For instance, the Rational technique generates a discharge of 514.53 m^3/second over a 2-year return period, but the Nakayasu SUH technique generates 617.01 m^3/second. A comparison of the anticipated flood discharge estimates using the two approaches for different return periods is shown in Table 11.

Table 11: Nakayasu SUH Flood Design.

Return Period [year]	**Q [m³/S]**	
	Rational	**Nakayasu SUH**
2	514.53	617.01
5	615.56	773.12
10	676.18	871.30
25	741.17	985.77
50	796.96	1,087.33
100	846.04	1,178.67

The difference in results between the two methods indicates that the Nakayasu SUH method is more sensitive to the physical variables of the watershed, such as concentration time and runoff shape, which leads to higher peak discharge estimates. This makes the Nakayasu SUH method more representative for complex hydrological conditions or watersheds with fast response times, which is the time it takes for the watershed to respond to rainfall and convert it into surface runoff in the form of peak discharge. Therefore, in flood control infrastructure planning, the results from the Nakayasu SUH method can be used as a conservative scenario to increase the safety margin of the design, particularly for structures intended to protect densely populated areas or critical assets.

As the return period increases, the predicted flood discharge values determined using the Nakayasu SUH approach exhibit an increasing trend. In a 100-year return period, the maximum discharge measured was 1,178.67 m³/second, while in a 2-year return period, the lowest discharge was 617.01 m³/second. To better comprehend how the discharge pattern changes with the return period, the relationship between the projected flood discharge and the return length is visually shown. Fig. 4 displays a graph of peak discharge estimates using the Nakayasu SUH method across different return periods. The chart shows an increasing trend, highlighting the method's sensitivity to extreme hydrological events and its application in designing flood control structures.

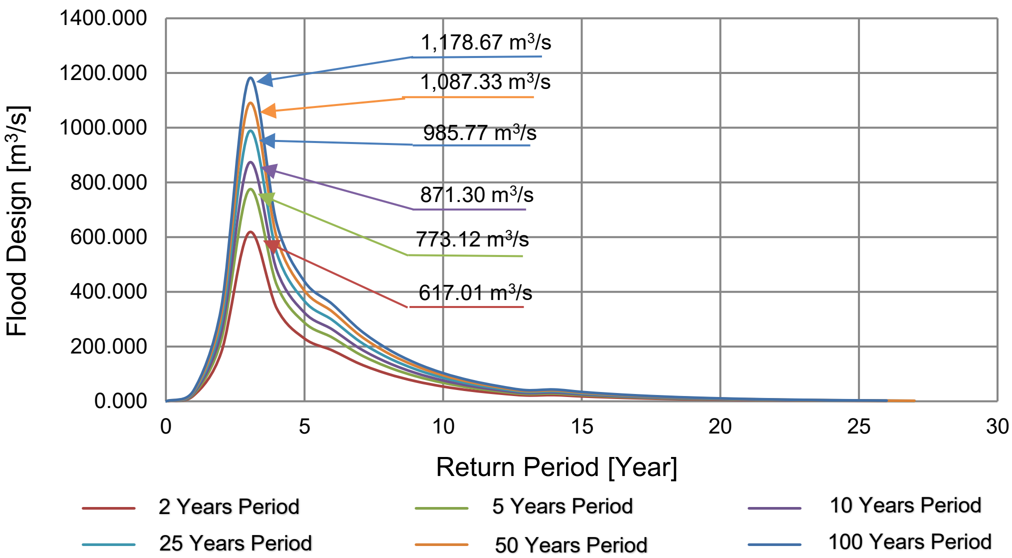

Fig. 4: Nakayasu SUH Chart.

Graphical depiction emphasizes that as the return period increases, the potential peak flood discharge that needs to be anticipated also becomes higher. This pattern of increase is crucial for reference in planning the capacity of flood control structures, as it reflects the level of hydrological risk across different event scenarios. This information is also valuable in the decision-making process that takes into account the tolerance limits for damage due to extreme flooding. Therefore, the graph in Fig 6 serves as a strategic analytical tool in supporting risk-based design.

Assessing the reservoir's capacity to handle the anticipated flood discharge is the next stage in the flood design study carried out using the Rational and Nakayasu SUH methodologies. The reservoir filling time for each return period was calculated using the projected flood discharge estimates from the Nakayasu SUH technique. The results indicate that as flood discharge increases, the time needed to fill the reservoir's storage volume decreases. For instance, during a 2-year return period with a discharge of 617.01 m³/s, the filling time is 39.31 seconds, whereas in a 100-year return period with a discharge of 1,178.67 m³/s, it reduces to 20.58 seconds. Complete details of these calculations are provided in Table 12.

Table 12: Reservoirs Filling Time.

Return Period [year]	2	5	10	25	50	100
Q [m^3/s]	617.01	773.12	871.30	985.77	1,087.33	1,178.67
Time to fill [s]	39.31	31.38	27.84	24.61	22.31	20.58

The difference in reservoir filling times based on return periods reflects the importance of having sufficient storage capacity to manage increasingly higher peak flood discharges. Shorter filling times indicate the need for a reservoir that can accommodate a larger volume or has a faster outflow capacity to prevent overflow. Therefore, evaluating the reservoir filling time is crucial in designing a reservoir that effectively reduces flood risks and ensures that the water management system operates optimally.

5 Conclusions

This study demonstrates that the nine reservoirs located in the upstream area of the Kuranji River Watershed namely PNP (2,418 m³), LPPM (445 m³), Arsip 1 (1,392 m³), Arsip 2 (522 m³), Arsip 3 (1,106 m³), Nurul Ilmi 1 (1,141 m³), Nurul Ilmi 2 (1,176 m³), Siratal Mustakim 1 (1,653 m³), and Siratal Mustakim 2 (14,400 m³) collectively provide a total storage capacity of 24,258 m³. Among them, Siratal Mustakim 2 is the largest and plays a pivotal role in flood mitigation efforts in the watershed. These reservoirs play a significant role in enhancing water resource management and mitigating flood risks in urban areas with steep topography, such as Padang City. Hydrological analysis, supported by statistical tests (Chi-Square and Kolmogorov–Smirnov) and advanced modeling techniques including the Rational Method, Nakayasu SUH, provides a more comprehensive understanding of rainfall-runoff behavior in the study area.

The extremely short filling time (e.g., 39.31 seconds during a 2-year return period) indicates that the reservoirs respond almost instantaneously to incoming flow. This rapid response underscores the critical need for effective overflow management strategies, including the integration of real-time flow monitoring, early warning systems, and automated outflow control to reduce the risk of overtopping and downstream flooding. Moreover, structural measures such as emergency spillways and adequate freeboard design must be incorporated to safely manage sudden inflow surges. This also highlights the necessity of complementing reservoir-based flood control in the Kuranji Watershed with upstream infiltration enhancement and downstream flow-routing infrastructure to delay and attenuate peak discharges. Hence, filling time should be interpreted as an initial indicator of watershed responsiveness, not a definitive measure of flood mitigation performance. A more comprehensive evaluation of flood attenuation capacity requires flow routing simulations that dynamically capture the inflow–outflow relationship over time.

Furthermore, this research is among the first to integrate long-term rainfall data with hydrological modeling for reservoir capacity planning in a tropical urban watershed. This integration enables more reliable flood forecasting and infrastructure design, providing a valuable reference for future water management strategies in regions affected by rapid urbanization and climate variability. In conclusion, the development and optimization of reservoirs in the Kuranji River Watershed represent a strategic effort to reduce flood hazards, ensure water availability, and support resilient, adaptable, and sustainable flood control infrastructure in tropical urban environments.

References

[1] Q. LU et al., “Multi-objective risk analysis for flood control operation of a complex reservoir system under multiple time-space correlated uncertainties,” J Hydrol (Amst), vol. 606, no. 1, p. 127419, 2022, doi: 10.1016/j.jhydrol.2021.127419.

[2] T. WANG et al., “Rank classification method for cascade reservoirs considering scale, benefits, and risk consequences,” J Hydrol (Amst), vol. 623, no. June, p. 129856, 2023, doi: 10.1016/j.jhydrol.2023.129856.

[3] I. A. ELSHINNAWY AND A. H. ALMALIKI, “Reservoir hydrologic routing for the hydrodynamic of Al-Manzala Lake, Egypt,” International Journal of GEOMATE, vol. 21, no. 83, pp. 157–165, 2021, doi: 10.21660/2021.83.j2117.

[4] K. KHASANOV, “A comprehensive analysis of reservoir capacity loss: A case study of the Akhangaran reservoir, Uzbekistan,” Water Cycle, vol. 6, no. March, pp. 105–117, 2025, doi: 10.1016/j.watcyc.2024.11.003.

[5] N. F. A. M. HUSSIN et al., "Rainfall Prediction Using Statistical Downscaling Based on Support Vector Machine in Selangor," Int J Adv Sci Eng Inf Technol, vol. 15, no. 1, pp. 345–352, 2025, doi: 10.18517/ijaseit.15.1.12410.

[6] D. K. HANH, D. D. TRUONG, AND K. T. T. BUI, "Application of Numerical Modeling and GIS for Simulating Inundation Under Dam Failure Scenarios," Civil and Environmental Engineering, vol. 20, no. 1, pp. 233–254, 2024, doi: 10.2478/cee-2024-0019.

[7] S. I. M. ABD ELRAHMAN AND I. M. I. ATAALMANAN, "Determination of the Hydrological and Morphometric Characteristics Using GIS," Civil and Environmental Engineering, vol. 19, no. 1, pp. 39–47, 2023, doi: 10.2478/cee-2023-0004.

[8] T. CHAITONGRAT, S. LIWTHAISONG, P. AKSORN, W. KUSONKHUM, AND N. LEUNGBOOTNAK, "Causal Relationship Model of Problems in Public Sector Procurement," International Journal of GEOMATE, vol. 20, no. 80, pp. 52–58, 2021, doi: 10.21660/2021.80.6266.

[9] PARAMASHANTI, RILDOVA, M. F. HERMANTO, AND N. NANDALIANADHIRA, "Determination of Lrfd Environmental Load Factors of Offshore Platform in the North of Java Sea and Makassar Strait," International Journal of GEOMATE, vol. 25, no. 111, pp. 94–103, 2023, doi: 10.21660/2023.111.4010.

[10] D. ÖZONUR, E. GÖKPINAR, F. GÖKPINAR, H. BAYRAK, AND H. H. GÜL, "Comparisons of the goodness of fit tests for the geometric distribution," Gazi University Journal of Science, vol. 26, no. 3, pp. 369–375, 2013.

[11] X. ZENG, D. WANG, AND J. WU, "Evaluating the Three Methods of Goodness of Fit Test for Frequency Analysis," Journal of Risk Analysis and Crisis Response, vol. 5, no. 3, p. 178, 2015, doi: 10.2991/jrarc.2015.5.3.5.

[12] B. OSENI AND F. AYOOLA, "Fitting the Statistical Distribution for Daily Rainfall in Ibadan, Based on Chi-Square and Kolmogorov-Smirnov Goodness-of-Fit," European Journal of Business and …, vol. 4, no. 17, pp. 62–70, 2012.

[13] M. MARSELINA, S. A. NURHAYATI, AND S. L. PANDIA, "Flood Analysis and Estimating Economic Losses in an Affected Area (Case Study: Cikapundung Watershed)," Air, Soil and Water Research, vol. 15, 2022, doi: 10.1177/11786221221131277.

[14] W. WAN, Y. LIU, H. ZHENG, J. ZHAO, F. ZHAO, AND Y. LU, "Optimization of Multi-Reservoir Flood Control Operating Rules: A Case Study for the Chaobai River Basin in China," Water (Switzerland), vol. 15, no. 15, 2023, doi: 10.3390/w15152817.

[15] D. MONTANARI et al., "Contour map of the top of the regional geothermal reservoir of Sicily (Italy)," J Maps, vol. 11, no. 1, pp. 13–24, 2015, doi: 10.1080/17445647.2014.935503.

[16] X. ZHAO, H. LI, Q. CAI, Y. PAN, AND Y. QI, "Managing Extreme Rainfall and Flooding Events: A Case Study of the 20 July 2021 Zhengzhou Flood in China," Climate, vol. 11, no. 11, 2023, doi: 10.3390/cli11110228.

[17] A. SUHARYANTO, "Estimating Flood Inundation Depth along the Arterial Road Based on the Rainfall Intensity," Civil and Environmental Engineering, vol. 17, no. 1, pp. 66–81, 2021, doi: 10.2478/cee-2021-0008.

[18] K. L. VOON, K. W. TAN, AND K. S. CHIN, "Assessment of the Flood and Drought Occurrence Using Statistically Downscaled Local Climate Models: a Case Study in Langat River Basin, Malaysia," f Environmental Engineering, vol. 18, no. 1, pp. 221–233, 2022, doi: 10.2478/cee-2022-0021.

[19] ELLITAN, "Best–fit Probability distribution model for peak daily rainfall of selected Cities in Nigeria," Экономика Региона, vol. 19, no. 19, p. 19, 2009.

[20] M. A. ALAM, K. EMURA, C. FARNHAM, AND J. YUAN, "Best-fit probability distributions and return periods for maximum monthly rainfall in Bangladesh," Climate, vol. 6, no. 1, 2018, doi: 10.3390/cli6010009.

[21] I. KOTLARSKI, "On characterizing the gamma and the normal distribution," Pac J Math, vol. 20, no. 1, pp. 69–76, 1967, doi: 10.2140/pjm.1967.20.69.

[22] R. MONTES-PAJUELO, Á. M. RODRÍGUEZ-PÉREZ, R. LÓPEZ, AND C. A. RODRÍGUEZ, "Analysis of Probability Distributions for Modelling Extreme Rainfall Events and Detecting Climate Change: Insights from Mathematical and Statistical Methods," Mathematics, vol. 12, no. 7, pp. 1–24, 2024, doi: 10.3390/math12071093.

[23] H. LIN, L. LIU, AND Z. ZHANG, "Hedging and evaluating tail risks via two novel options based on type II extreme value distribution," Symmetry (Basel), vol. 13, no. 9, pp. 1–18, 2021, doi: 10.3390/sym13091630.

[24] H. H. HASAN, S. F. M. RAZALI, A. Z. I. A. ZAKI, AND F. M. HAMZAH, "Integrated hydrological-hydraulic model for flood simulation in tropical urban catchment," Sustainability (Switzerland), vol. 11, no. 23, pp. 1–24, 2019, doi: 10.3390/su11236700.

[25] S. A. LONE, T. N. SINDHU, M. K. H. HASSAN, T. A. ABUSHAL, S. ANWAR, AND A. SHAFIQ, "Theoretical Structure and Applications of a Newly Enhanced Gumbel Type II Model," Mathematics, vol. 11, no. 8, 2023, doi: 10.3390/math11081797.

[26] R. PERMATASARI, D. K. NATAKUSUMAH, AND A. SABAR, "Determining peak discharge factor using synthetic unit hydrograph modelling (case study: Upper komering South Sumatera, Indonesia)," International Journal of GEOMATE, vol. 13, no. 36, pp. 1–5, 2017, doi: 10.21660/2017.36.2744.

[27] A. VIGLIONE, R. MERZ, AND G. BLÖSCHL, "On the role of the runoff coefficient in the mapping of rainfall to flood return periods," Hydrol Earth Syst Sci, vol. 13, no. 5, pp. 577–593, 2009, doi: 10.5194/hess-13-577-2009.

[28] T. BLUME, E. ZEHE, AND A. BRONSTERT, "Rainfall-runoff response, event-based runoff coefficients and hydrograph separation," Hydrological Sciences Journal, vol. 52, no. 5, pp. 843–862, 2007, doi: 10.1623/hysj.52.5.843.

[29] A. N. ANNA et al., "Spatial Modelling of Local Flooding for Hazard Mitigation in Surakarta, Indonesia," International Journal of GEOMATE, vol. 21, no. 87, pp. 145–152, 2021, doi: 10.21660/2021.87.j2306.

[30] M. KENCANAWATI, D. IRANATA, AND M. A. MAULANA, "Hydrologic Modeling System HEC-HMS Application for Direct Runoff Determination," Journal of Human, Earth, and Future, vol. 4, no. 2, pp. 153–165, 2023, doi: 10.28991/HEF-2023-04-02-02.

[31] I. FLORES-MONTOYA, Á. SORDO-WARD, L. MEDIERO, AND L. GARROTE, "Fully stochastic distributed methodology for multivariate flood frequency analysis," Water (Switzerland), vol. 8, no. 6, 2016, doi: 10.3390/w8060225.

[32] ANDRIANI, B. ISTIJONO, APRISAL, T. OPHIYANDRI, AND T. H. A. PUTRA, "Optimization of Land Use To Reduce Surface Runoff and Erosion in Kuranji Watershed," International Journal of GEOMATE, vol. 22, no. 90, pp. 102–109, 2022, doi: 10.21660/2022.90.j2310.

[33] M. SAFRIANI, A. AMIR, AND M. F. IKHWALI, "Evaluation of Krueng Tripa River Capacity in Ujung Krueng Village, Nagan Raya Regency, Indonesia," IOP Conf Ser Earth Environ Sci, vol. 1203, no. 1, 2023, doi: 10.1088/1755-1315/1203/1/012033.

[34] R. KARAMMA, S. BADARUDDIN, R. MUSTAMIN, AND Z. SAING, "Flood Modelling due to Dam Failure Using HEC-RAS 2D with GIS Overlay: Case Study of Karalloe Dam in South Sulawesi Province Indonesia," Civil Engineering and Architecture, vol. 10, no. 7, pp. 2833–2846, 2022, doi: 10.13189/cea.2022.100704.

[35] SARINO, D. D. A. PUTRANTO, A. L. YUONO, AND I. C. JULIANA, "Database Structure of Land Allocation Management Information System for Estimating Run-Off in Watersheds," International Journal of GEOMATE, vol. 17, no. 59, pp. 34–42, 2019, doi: 10.21660/2019.59.4710.

[36] M. B. ANSORI, U. LASMINTO, AND A. A. G. KARTIKA, "Flood Hydrograph Analysis Using Synthetic Unit Hydrograph, Hec-Hms, and Hec-Ras 2D Unsteady Flow Precipitation on-Grid Model for Disaster Risk Mitigation," International Journal of GEOMATE, vol. 25, no. 107, pp. 50–58, 2023, doi: 10.21660/2023.107.3719.